2.5-D finite-difference solution of the acoustic wave equation

Amélia Novais and Lúcio T. Santos

email: *amelia@ime.unicamp.br*
keywords: *finite difference, stability, wave*

ABSTRACT

Finite differences applied to the full 3-D wave equation is a rather time consuming process. However, in the 2.5-D situation, we can take advantage of the medium symmetry. By taking the Fourier transform with respect to the out-of-plane direction (symmetry axis), the 3-D problem can be reduced to a repeated 2-D one. The third dimension is taken in to account by a sum over the corresponding wave vector component. A criterion where to end this theoretically infinite sum derives from stability conditions of the employed FD schemes. In this way, the finite differences calculations can be accelerated by a factor that increases with the size of the model. Even for relatively small models, this procedure reduces the computation time by a factor of about ten. The modeling results obtained by this 2.5-D finite-difference scheme are of comparable quality to a standard 3-D finite-difference scheme.

INTRODUCTION

Finite Difference (FD) modeling of wave propagation in heterogeneous media is a useful technique in a number of disciplines, including seismology and ocean acoustics, among others. However, the size of the models that can be treated by finite difference methods in three spatial dimensions has been rather limited, except possibly, on supercomputers.

In other forward modeling schemes, the medium symmetry in the so-called 2.5-D situation has been made use of in order to reduce the computational costs. The attribute 2.5-D designates a situation where the medium depends on two spatial coordinates only, and the seismic line is orthogonal to the symmetry axis.

In Song & Williamson (1995) the authors have shown how a finite difference scheme can be adapted to the 2.5-D situation. They reduce the full 3-D finite-difference scheme to a repeated 2-D FD scheme by applying the Fourier transform with respect to the out-of-plane coordinate to the 3-D wave equation and using the medium symmetry. The resulting 2-D equation in the frequency domain is then solved by a finite difference scheme. The full 3-D wavefield is finally reconstructed by realizing a inverse Fourier transform as a sum from 0 to the critical wavenumber. To validate the method, they compare the numerical solution with the analytic solution for a homogeneous medium. For an inhomogeneous medium, the comparison was with the 2.5-D FD solution and the Born approximation (which is know to underestimate amplitudes).

Zhou & Greenhalgh (1998) presented a similar approach, using, however, a finite element method in the frequency domain to compute the numerical solution for the resulting 2-D equation, with 2.5-D boundary conditions. The frequency domain solution has a small error in the neighborhood of the source. They suspected that possible reasons for the error are the finite sampling of the wavenumber and the exclusion of the evanescent field (post-critical reflection).

An idea similar to Song & Williamson's was present by Cao & Greenhalgh (1998). They compute the stability condition for the resulting 2-D equation to control the size in time. Again, the sum for the inverse Fourier transform is carried out up to the critical wavenumber. The numerical comparison is done only for homogeneous media.

In this work, we apply the 2.5-D FD method in the time domain rather than in the frequency domain. In this way, the numerical errors due to the wrapping of the temporal Fourier transform reported by Song & Williamson (1995) are avoided. Moreover, the inverse Fourier transform is realized by a simple sum over all 2-D finite-difference results in order to obtain the full 3-D wavefield. Of course, it is computationally impossible to realize an infinite sum. We apply the von Neumann criterion for stability of the 2-D equation and use the stability condition of the 3-D finite difference scheme of Mufty (1990). In this way, we obtain a criterion where to stop the summation. We validate our approach for inhomogeneous media by a comparison with 3-D finite difference modeling.

THE 2.5-D SOLUTION

We assume that the 3-D seismic wave propagation is governed by the acoustic wave equation with constant density

$$u_{xx} + u_{yy} + u_{zz} = \frac{1}{v^2} u_{tt} - f(t)\delta(x - x_s)\delta(y - y_s)\delta(z - z_s) \ , \tag{1}$$

where $u \equiv u(x, y, z, t)$ is the acoustic wavefield, $v \equiv v(x, y, z)$ is the velocity field, $f(t)$ is a band-limited source, and (x_s, y_s, z_s) is the source location.

We assume that the velocity field is a function of x and z only, i.e., $v \equiv v(x, z)$, and that the source is located in the symmetry plane ($y_s = 0$). This is the so-called 2.5-D situation. Applying the Fourier transform in the out-of-plane direction (y-coordinate), the 3-D wave equation (1) can be reduced to the following one

$$U_{xx} - \kappa^2 U + U_{zz} = \frac{1}{v^2} U_{tt} - f(t)\delta(x - x_s)\delta(z - z_s) \ , \tag{2}$$

where

$$U \equiv U(x, \kappa, z, t) = \int_{-\infty}^{\infty} dy \ u(x, y, z, t) \ e^{-i\kappa y} \ , \tag{3}$$

and κ is the wavenumber for the y-direction. Solving the 2-D equation (2) using a finite-difference scheme for a discrete set of equally spaced κ's, $\kappa_j = j\Delta\kappa$, the solution at $y = 0$ is then obtained by an inverse Fourier transform, which can be approximated by

$$u(x, 0, z, t) = \frac{1}{2\pi} \int_{-\infty}^{\infty} d\kappa \ U(x, \kappa, z, t) \ e^{i\kappa 0} \approx \frac{\Delta\kappa}{\pi} \sum_{k_j \geq 0} U(x, \kappa_j, z, t) \ , \tag{4}$$

where we have used the fact that $U(x, \kappa, z, t)$ is an even function in κ. Equation (4) means that the field $u(x, 0, z, t)$ can be obtained by summing the contributions for all $\kappa_j \geq 0$.

FINITE-DIFFERENCE FORMULAS

A set of indices m, n and l is chosen to establish a finite-difference scheme with uniform grid spacing Δx, Δz and Δt in x, z and t, respectively: $x_m = x_{\min} + m \ \Delta x$, $z_n = z_{\min} + n \ \Delta z$ and $t_l = t_{\min} + l \ \Delta t$. Consequently, we denote, for a fixed κ, $U(x_m, \kappa, z_n, t_l) = U^l_{m,n}$.

The finite-difference scheme for solving equation (2) was chosen to be fourth-order in space and second-order in time (Strikwerda, 1989), and is given by

$$\begin{aligned} U^{l+1}_{m,n} \ = \ & -\alpha_{m,n} \left[U^l_{m-2,n} + U^l_{m+2,n} - 16 \left(U^l_{m-1,n} + U^l_{m+1,n} \right) + 30 U^l_{m,n} \right] \\ & -\beta_{m,n} \left[U^l_{m,n-2} + U^l_{m,n+2} - 16 \left(U^l_{m,n-1} + U^l_{m,n+1} \right) + 30 U^l_{m,n} \right] \\ & -v^2 \Delta t^2 \kappa^2 U^l_{m,n} + 2U^l_{m,n} - U^{l-1}_{m,n} + f^l_{m,n} \ , \end{aligned} \tag{5}$$

where

$$\alpha_{m,n} = \frac{v^2_{m,n}}{12} \frac{\Delta t^2}{\Delta x^2}, \quad \beta_{m,n} = \frac{v^2_{m,n}}{12} \frac{\Delta t^2}{\Delta z^2}, \tag{6}$$

$v_{m,n}$ denotes the velocity at (x_m, z_n), and

$$f^l_{m,n} = \begin{cases} f(t_l) \ , & x_m = x_s \text{ and } z_n = z_s, \\ 0 \ , & \text{otherwise.} \end{cases} \tag{7}$$

For initiating the propagation process, we set

$$U^0_{m,n} = 0, \text{ for all } m, n \ , \tag{8}$$

and define the boundary conditions

$$U^l_{m,0} = U^l_{0,n} = 0, \text{ for all } m, n, l \ . \tag{9}$$

We will consider a uniform grid spacing, i.e., $\Delta x = \Delta z = h$. For the scheme (5) to be stable (see Appendix A), we should have

$$\kappa^2 + \frac{32}{3\ h^2} \leq \left(\frac{2}{v\ \Delta t}\right)^2 \ , \tag{10}$$

and, since κ must be real, equation (10) provides a condition between Δt and h, viz.,

$$\Delta t \leq \sqrt{\frac{3}{8}} \frac{h}{v_{\max}} \ , \tag{11}$$

where $v_{\max}$ represents the maximum value of the velocity field.

We compare the numerical solution obtained by the process described above with the one obtained by a scheme of fourth-order in space and second-order in time for the full wave 3-D equation (1). For the 3-D scheme, we have that the maximum value of h, that can be used without causing excessive dispersion of energy, is determined by the following condition (Mufti, 1990)

$$h \leq \frac{v_{\min}}{\vartheta f_{\max}}. \tag{12}$$

Here, $v_{\min}$ is the minimum value of the velocity field, $f_{\max}$ is the maximum frequency of the source pulse, and ϑ is the number of samples per minimum wavelength (to be chosen). Moreover, for a given value of the grid spacing, the process becomes numerically unstable unless the time sampling interval satisfies the condition

$$\Delta t \leq \frac{\gamma\ h}{v_{\max}} \ , \tag{13}$$

where γ is a constant. According to Mufti et al. (1996), the optimal values for the above parameters for 3-D FD are $\gamma = 0.5$ and $\vartheta = 3.5$.

Now, if we use the 3-D condition (13), which is slightly stronger than the 2.5-D condition (11), in equation (10), we obtain

$$\kappa_{\max} \leq \frac{4\sqrt{3}}{3h}. \tag{14}$$

Condition (14) can be used as a stop criterion for the summation in equation (4). Note that condition (14) is stronger than a condition based on the Nyquist criterion (see, e.g., Brigham, 1988) that would require $\kappa_{\max} \leq \pi/h$. To determine the sampling rate for the wavenumber ($\Delta\kappa$), we have used the property of the discrete Fourier transform that $\Delta\kappa = \pi/(y_{\max} - y_{\min})$, where $[y_{\min}, y_{\max}]$ is the range in the out-of-plane direction to be covered.

NUMERICAL EXPERIMENTS

We illustrate the 2.5-D finite-difference process discussed above by means of two numerical experiments. The first model consists of a homogeneous layer between two homogeneous half-spaces (see Figure 1). The velocities, from top to bottom, are 3 m/ms, 3.5 m/ms, and 4 m/ms, respectively. For this model, we have simulated a split-spread experiment with a omnidirectional point source located at $x = 800$ m and 41 receivers equally spaced at every 40 m between $x = 0$ m and $x = 1600$ m.

Figure 2 shows the simulated seismic common-shot section resulting from the 2.5-D finite-difference scheme, together with the corresponding section obtained using a 3-D finite-difference scheme. In both schemes we have used a uniform spatial grid, $\Delta x = \Delta y = \Delta z = 10$ m, with time sampling interval $\Delta t = 1$ ms. The source wavelet was chosen to be a Küpper wavelet (Fuchs and Müller, 1971) with

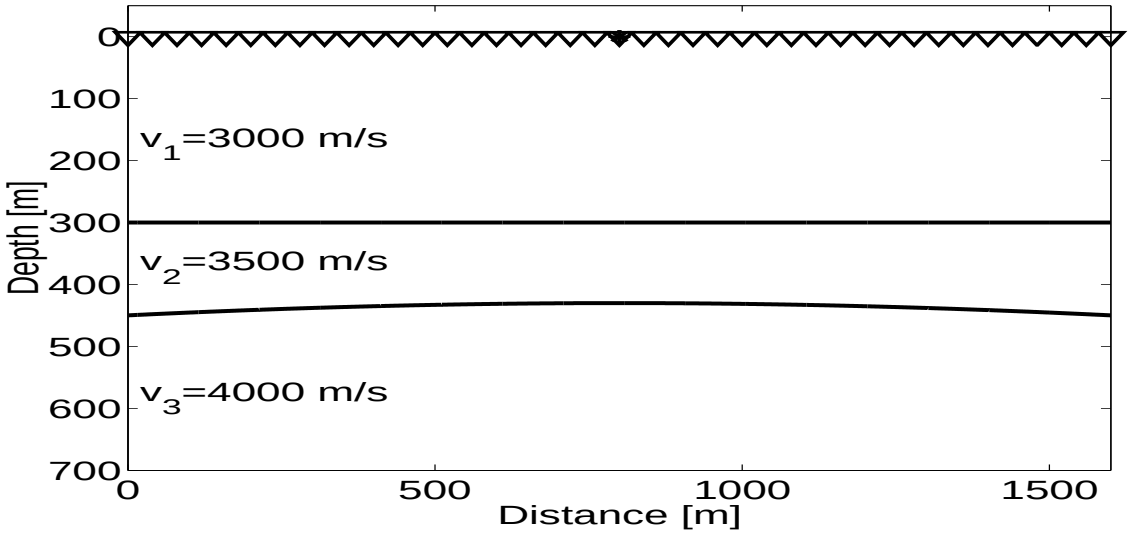

Figure 1: First model: Two interfaces, separating three homogeneous layers

$f_{\max}$ =35 Hz. For the summation indicated in equation (4) for the inverse Fourier transform, we take $\Delta\kappa = 0.0005\ \mathrm{m}^{-1}$ and $\kappa_{\max} = 0.22\ \mathrm{m}^{-1}$. All parameters used are clearly in accordance with the criteria described in the previous section. We observe in Figure 2 that both FD schemes yield the expected two reflection events with apparently identical kinematics (arrival time) and dynamics (amplitude). Note that the numerical noise reported by Song and Williamson (1995) for their frequency-domain scheme cannot be observed in the data in Figure 2, modeled by our time-domain scheme.

Since the two modeled sections in Figure 2 obtained by the 2.5-D and 3-D schemes look almost identical, we proceed with a comparison of some selected traces. Due to the symmetry of the model, the simulated seismic section is symmetric with respect to the source position. Therefore, we choose only traces recorded to the left of the source, at the positions $x = 0$ m, $x = 250$ m, $x = 550$ m, and $x = 800$ m. In the trace-by-trace comparison depicted in Figure 3, it is almost impossible to distinguish between the two modeling results. In Figure 4 we show the differences between the respective traces. Observe that the percentage error is smaller than 2.5%. So, for all practical purposes, the 2.5-D FD scheme is as accurate as the 3-D scheme.

The second model has also two interfaces (see Figure 5), and the velocities of the layers, from top to bottom, are 2.5 m/ms, 3 m/ms, and 3.5 m/ms, respectively.

As before, we have simulated a split-spread experiment with a omnidirectional point source located at $x = 0$ m and 61 receivers equally spaced at every 25 m between $x = -750$ m and $x = 750$ m. We have used the same discretization and wavelet as in the first experiment. In this situation, the recorded wavefield has encountered a caustic and a diffraction. In Figure 6 we show the common-shot section for both finite-difference schemes (2.5-D and 3-D). As for the first model, the simulated seismic sections are practically identical (kinematics and dynamicly).

For a better visualization, we compare in Figures 7 and 8 the modeled traces at $x = -750$m, $x = -550$m, $x = -350$m, $x = -150$m, $x = 75$m, $x = 300$m, $x = 525$m, and $x = 750$m. From this trace-by-trace comparison, we can observe that both the 2.5-D and 3-D FD schemes yield almost the same results for both the reflection and diffraction events (see, e.g., the trace at $x = 300$ m). Figures 9 and 10 show the differences between traces, where we observe that, again, the percentage error is always less the 2.5%.

CONCLUSIONS

We have used a similar approach of Song and Williamson (1995) to take advantage of the medium symmetry in the 2.5-D situation to accelerate the finite-difference computation of 3-D wave propagation. The full 3-D solution can be recovered as a summation of 2-D solutions of 2-D differential equations that are obtained from the original 3-D wave equation after the application of the Fourier transform in the y-direction.

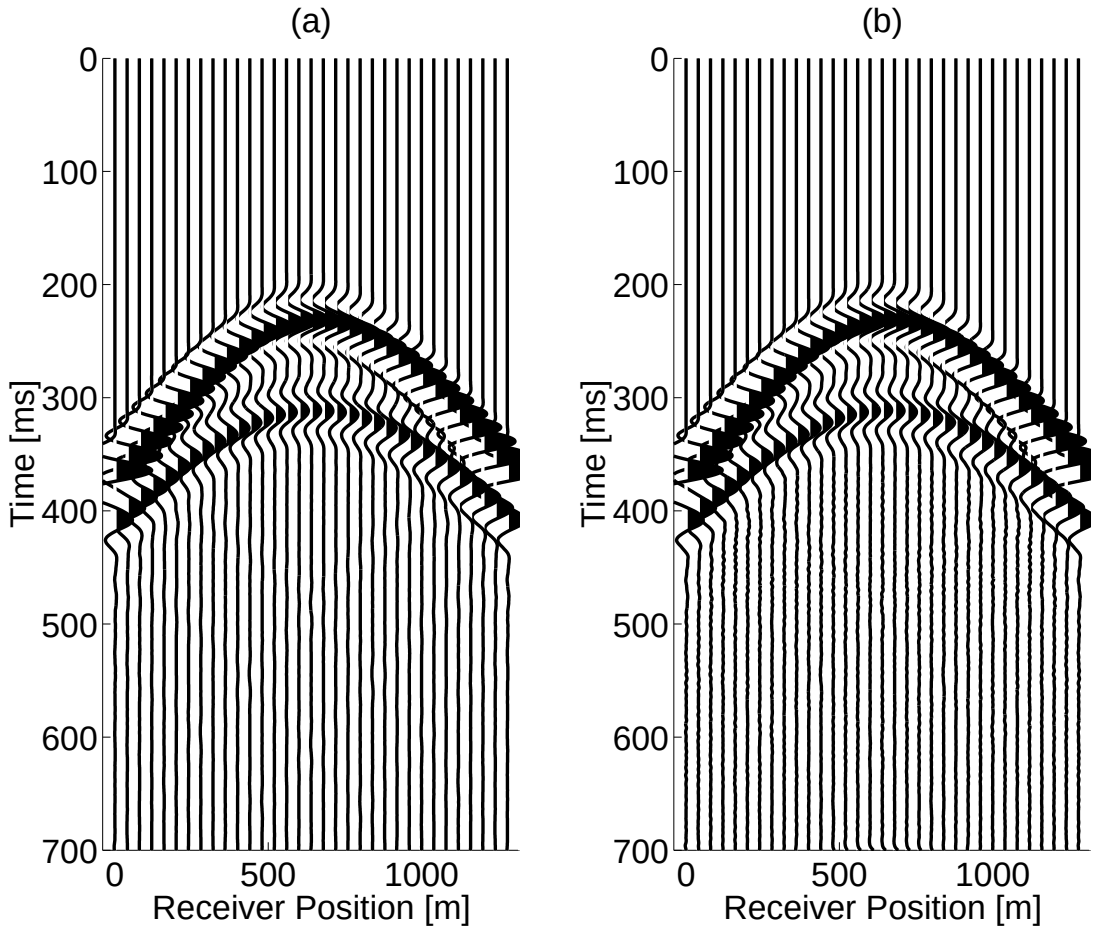

Figure 2: Synthetic seismograms (First Model): (a) 2.5-D FD. (b) 3-D FD.

In this way, the finite differences calculations can be accelerated by a factor that increases with the size of the model.

The numerical solutions of the wave equation have been computed by finite difference schemes of fourth-order in space and second-order in time. Our approach is developed in the time domain, unlike Song and Williamson (1995) who work in the frequency domain.

For simple models consisting of smooth reflectors between homogeneous acoustic media, we have compared the developed 2.5-D finite-difference scheme with the corresponding solution using a 3-D finite-difference scheme. We observed in all cases (two typical examples are shown in this paper) that the wavefield modeled by 2.5-D finite differences agrees very well with the 3-D results.

We have also derived a criterion about where to terminate the wavenumber summation that realizes the inverse Fourier transform of the modeled wavefield.

ACKNOWLEDGEMENTS

This work was kindly supported by FAPESP & CNPq (Brazil), and the sponsors of the *Wave Inversion Technology (WIT) Consortium* (Germany).

REFERENCES

Brigham, E. O. (1988). The fast Fourier transform and its applications. *Prentice-Hall, Inc*.

Cao, S. and Greenhalgh, S. (1998). 2.5-D modeling of seismic wave propagation: Boundary condition,

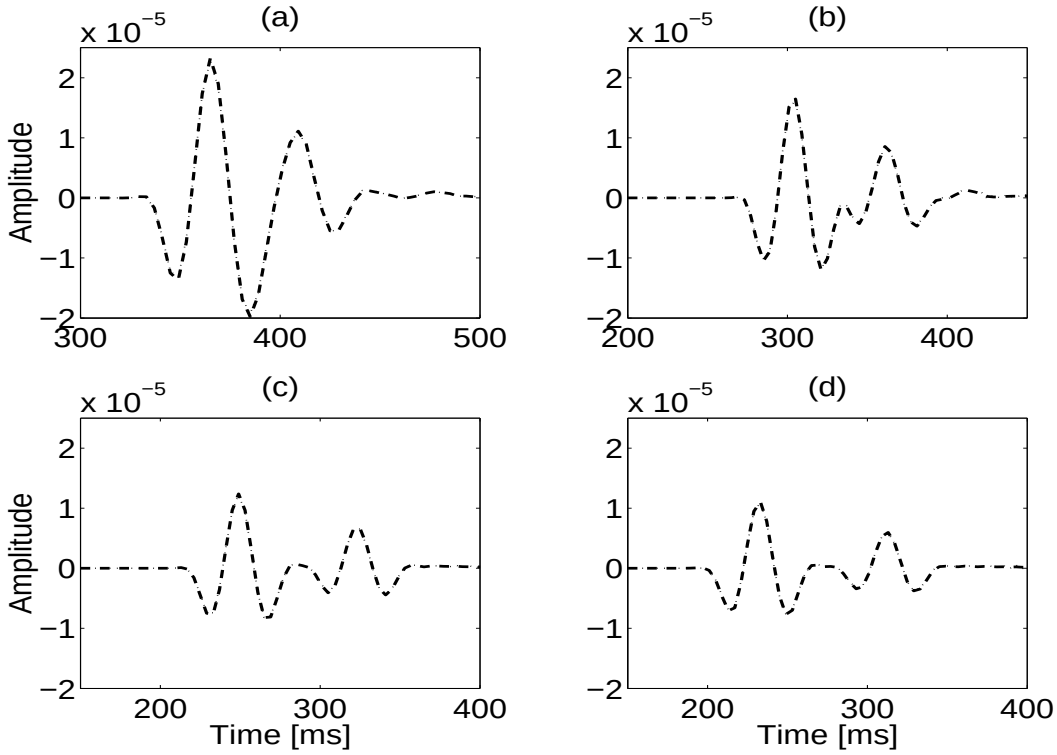

Figure 3: First model: Comparison of traces modeled by 2.5-D FD (dashed line) and 3-D FD (dotted line). Trace at (a) $x = 0$m, (b) $x = 250$m, (c) $x = 550$m and (d) $x = 800$m.

stability criterion, and efficiency. *Geophysics*, 63:2082–2090.

Fuchs, K. and Müller, G. (1971). Computation of synthetic seismograms with the reflectivity method and comparison with observations. *Geophys. J. R. Astr. Soc.*, 23(4):417–433.

Mufti, I. R. (1990). Large-scale three-dimensional seismic models and their interpretive significance. *Geophysics*, 55:1066–1182.

Mufti, I. R., Pita, J. A., and Huntley, R. W. (1996). Finite-difference depth migration of exploration-scale 3D seismic data. *Geophysics*, 61:776–794.

Song, Z. and Williamson, P. R. (1995). Frequency-domain acoustic-wave modeling and inversion of cross-hole date: Part I – 2.5-d. *Geophysics*, 60:784–795.

Strikwerda, J. C. (1989). Finite difference schemes and partial differential equations. *Wadsworth & Brook/Cole*.

Zhou, B. and Greenhalgh, S. A. (1998). Composite boundary-valued solution of the 2.5-d Green's function for arbitrary acoustic media. *Geophysics*, 63:1813–1823.

APPENDIX A

STABILITY CONDITIONS

In a similar way to Mufti (1990), we use the von Neumann criterion to obtain the stability condition for the FD scheme given by equation (5). That is, we substitute $U_{m,n} = \xi^l e^{i\,\kappa_x\,\Delta x} e^{i\,\kappa_y\,\Delta y}$ in equation (5) and obtain the amplification factor $\xi \equiv \xi(\kappa_x \Delta x, \kappa_z \Delta z)$, which is given by the solution of the following

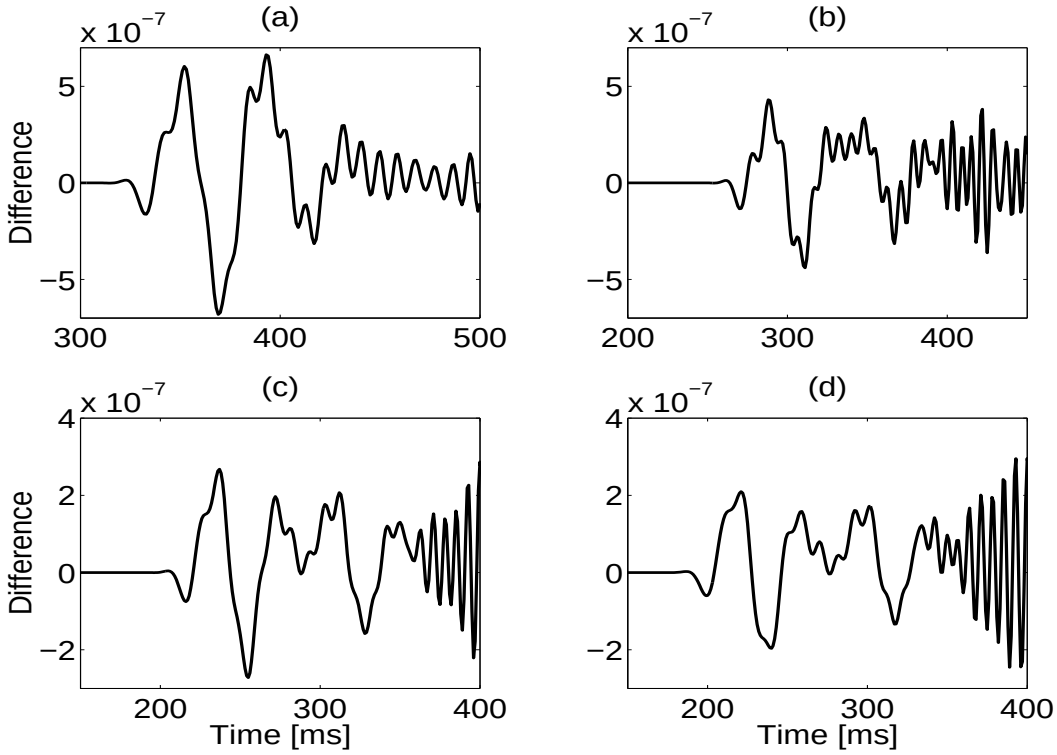

Figure 4: First model: Differences of traces modeled by 2.5-D FD (dashed line) and 3-D FD (dotted line). Trace at (a) $x = 0$m, (b) $x = 250$m, (c) $x = 550$m and (d) $x = 800$m.

quadratic equation

$$\begin{aligned}\xi^2 &= -\xi\left\{\alpha\left[(e^{-2i\kappa_x\Delta x}+e^{2i\kappa_x\Delta x})-16(e^{-i\kappa_x\Delta x}+e^{i\kappa_x\Delta x})+30\right]\right.\\ &\quad\left.+\beta\left[(e^{-2i\kappa_z\Delta z}+e^{2i\kappa_z\Delta_z})-16(e^{-i\kappa_z\Delta_z}+e^{i\kappa_z\Delta_z})+30\right]\right\}\\ &\quad+(v\ \kappa\ \Delta t)^2\xi+2\xi-1\ .\end{aligned} \tag{15}$$

Here, for simplicity, $\alpha = \alpha_{m,n}$, $\beta = \beta_{m,n}$ and $v = v_{m,n}$. The solution is easily computed as

$$\xi = \gamma \pm \sqrt{\gamma^2 - 1}\ , \tag{16}$$

where

$$\gamma = 1 - \frac{(v\ \kappa\ \Delta t)^2}{2} - 8\alpha\sin^2\frac{\kappa_x\Delta_x}{2}\left(3+\sin^2\frac{\kappa_x\Delta_x}{2}\right) - 8\beta\sin^2\frac{\kappa_z\Delta_z}{2}\left(3+\sin^2\frac{\kappa_z\Delta_z}{2}\right). \tag{17}$$

For stability, we must have $|\xi| \leq 1$ (Strikwerda, 1989), which implies $|\gamma| \leq 1$. If we use a uniform grid, i.e., $\Delta x = \Delta z = h$, this condition reduces to

$$0 \leq \frac{(v\ \kappa\ \Delta t)^2}{2} + \frac{2}{3}\frac{v^2\ \Delta t^2}{h^2}[(3+\sin^2\theta)\sin^2\theta + (3+\sin^2\phi)\sin^2\phi] \leq 2\ , \tag{18}$$

where

$$\theta = \frac{\kappa_x\Delta x}{2}\ , \quad \text{and} \quad \phi = \frac{\kappa_z\Delta z}{2}\ . \tag{19}$$

The left-hand side of inequality (18) is clearly satisfied. The maximum of the above expression occurs when $\sin^2\theta = \sin^2\phi = 1$. Using these values in the right-hand-side of inequality (18), we obtain the following condition for κ, Δt and h,

$$\kappa^2 + \frac{32}{3h^2} \leq \left(\frac{2}{v\Delta t}\right)^2\ . \tag{20}$$

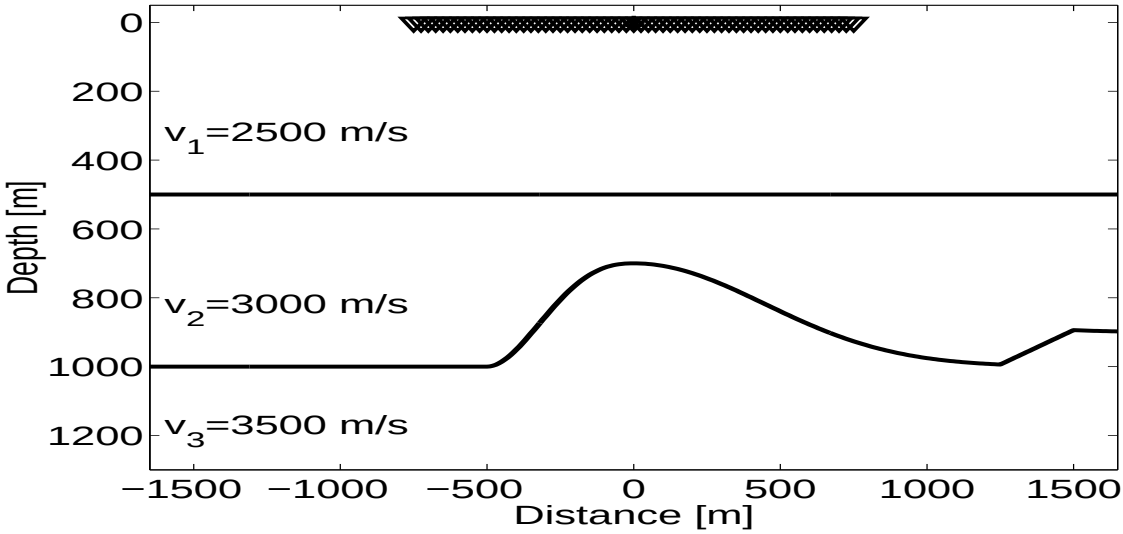

Figure 5: Second Model: two interfaces, separating three homogeneous layers

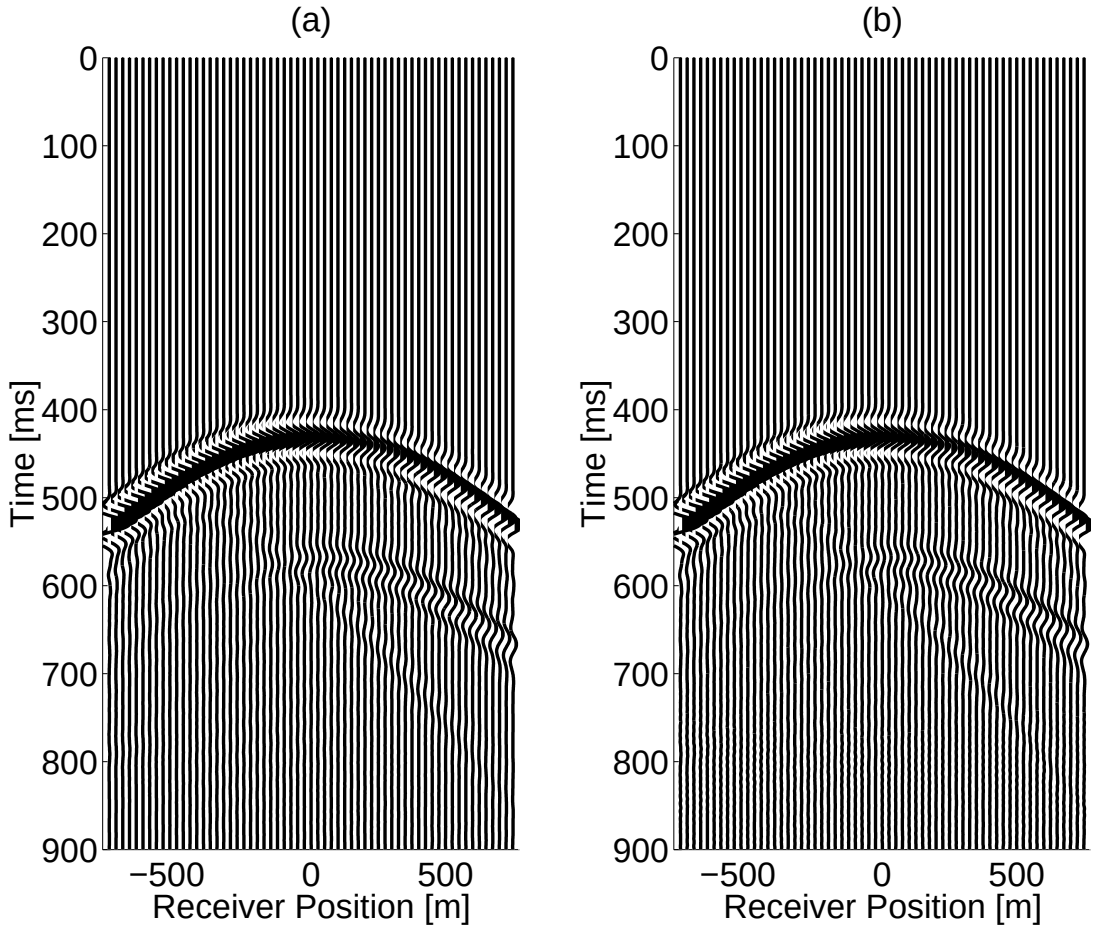

Figure 6: Synthetic seismograms (Second Model): (a) 2.5-D FD. (b) 3-D FD.

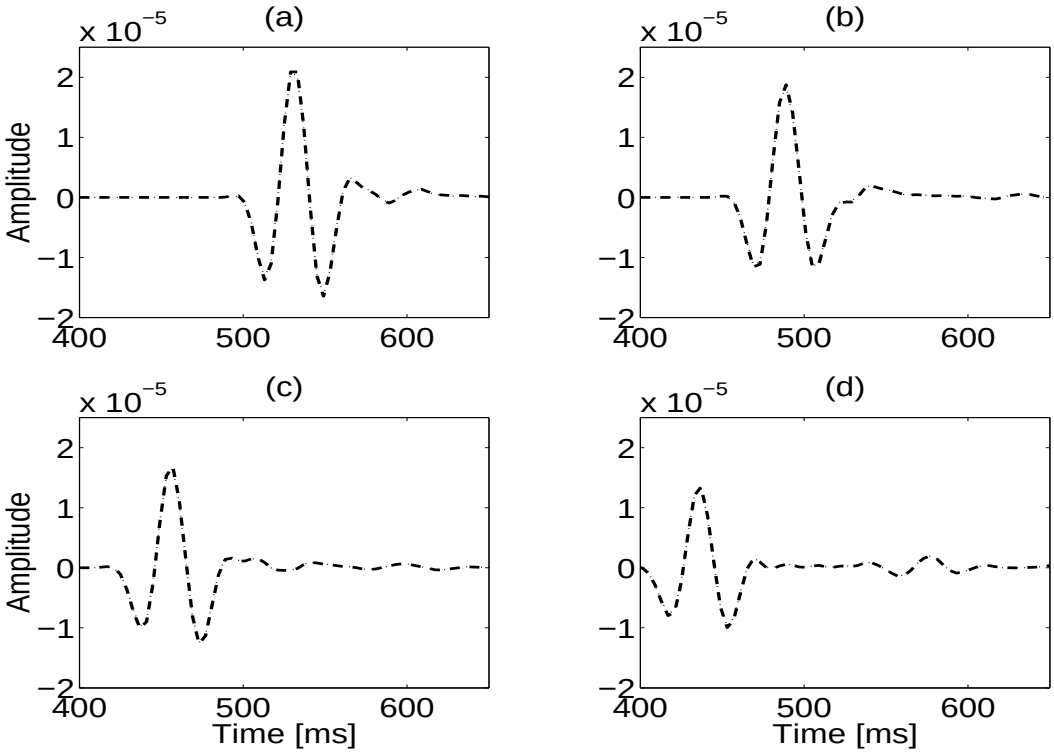

Figure 7: Second model: Comparison of traces modeled by 2.5-D FD (dashed line)and 3-D FD (dotted line). Trace at (a) $x = -750$m, (b) $x = -550$m, (c) $x = -350$m and (d) $x = -150$m.

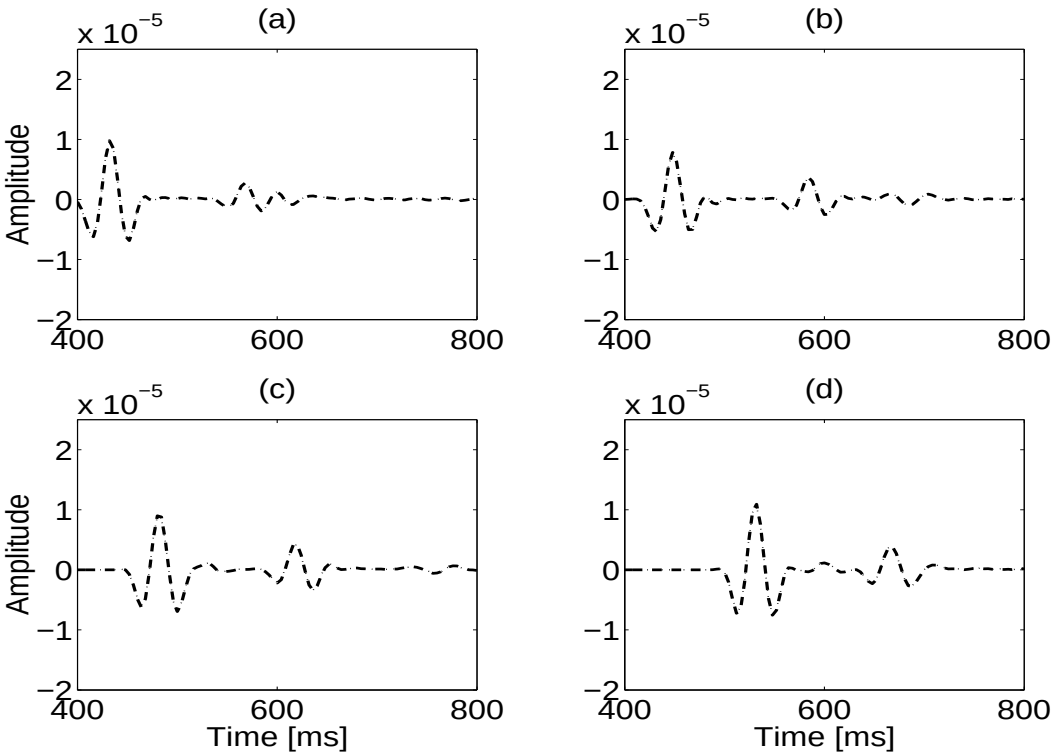

Figure 8: Second model: Comparison of traces modeled by 2.5-D FD (dashed line)and 3-D FD (dotted line). Trace at (a) $x = 75$m, (b) $x = 300$m, (c) $x = 525$m and (d) $x = 750$m.

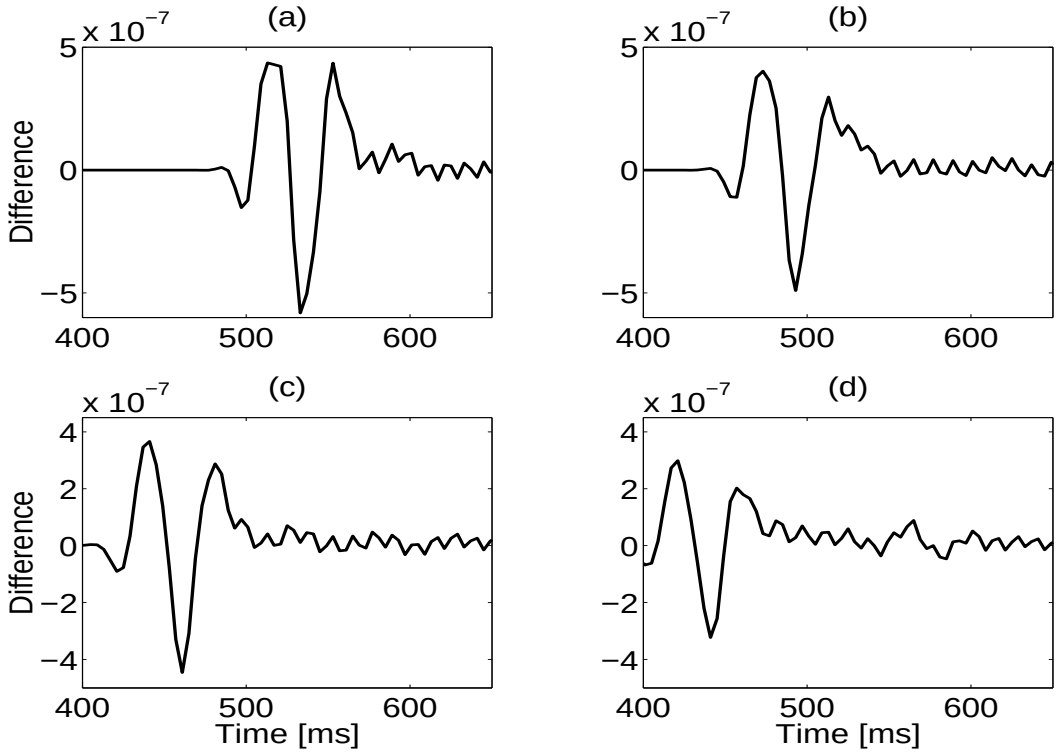

Figure 9: Second model: Difference of traces modeled by 2.5-D FD and 3-D FD. Trace at (a) $x = -750$m, (b) $x = -550$m, (c) $x = -350$m and (d) $x = -150$m.

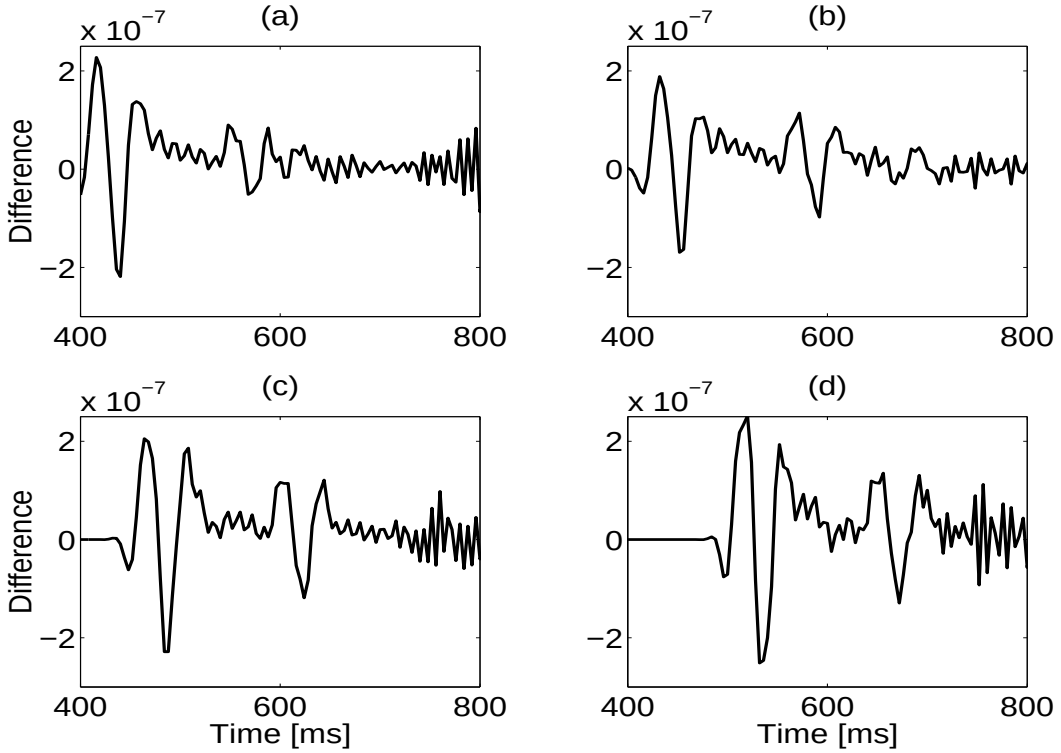

Figure 10: Second model: Difference of traces modeled by 2.5-D FD and 3-D FD. Trace at (a) $x = 75$m, (b) $x = 300$m, (c) $x = 525$m and (d) $x = 750$m.